Article ID: 1006-8775(2020) 04-0390-12

The Impact of Assimilating FY−3C GNOS GPS Radio Occultation Observations on GRAPES Forecasts

WANG Jin-cheng (王金成), GONG Jian-dong (龚建东), HAN Wei (韩 威)
(1. Numerical Weather Prediction Center, China Meteorological Administration, Beijing 100081 China;
2. National Meteorological Center, China Meteorological Administration, Beijing 100081 China)

Abstract: In the present study, a gross quality control (QC) procedure is proposed for the Global Navigation Satellite System Occultation Sounder (GNOS) Global Positioning System radio occultation (GPS RO) refractivity data to remove abnormal data before they are assimilated. It consists of a climate extreme check removing data outside the range of the Constellation Observing System for Meteorology, Ionosphere and Climate (COSMIC) climate maxima and minima over approximately five years, and a vertical gradient check that rejects profiles containing super-refractions. These two QC steps were applied sequentially to identify outliers in GNOS GPS RO refractivity data during boreal winter 2013/2014. All of the abnormal refractivity profiles and the outliers at each level of the GNOS GPS RO observations were effectively removed by the proposed QC procedure. The post-QC GNOS GPS RO refractivity observations were then assimilated in the Global/Regional Analysis and PrEdiction System (GRAPES) using the three-dimensional variational (3D-Var) system. The impacts of the GNOS refractivity observation on GRAPES analysis and forecasting were evaluated and analyzed using an observation system experiment run over one whole winter season of 2013/2014. The experiment results demonstrated a positive impact of GNOS GPS RO data on analysis and forecast quality. The root mean squared error of GRAPES analysis temperature was reduced by 1% in the Southern Hemisphere (SH) extratropics and in the tropics, and the anomaly correlation scores of the forecasted 500-hPa geopotential height over the SH increased significantly during days 1 to 5. Overall, the benefits of using GNOS GPS RO data are significant in the SH and tropics.

Key words: GNOS; FY-3C; GPS RO; Global NWP; data assimilation; GRAPES
CLC number: P456.7 **Document code:** A
https://doi.org/10.46267/j.1006-8775.2020.034

1 INTRODUCTION

Global Positioning System (GPS) radio occultation (RO) observations have become one of the most important components of the global observing system assimilated in global operational numerical weather prediction (NWP) systems (Eyre [1]; Cucurull et al. [2-4]; Buontempo et al. [5]; Anlauf et al. [6]; Rennie [7]; Healy [8]; Cucurull [9]; Poli et al. [10]; Cardinali et al. [11]; Liu et al. [12]) since the Constellation Observing System for Meteorology, Ionosphere and Climate (COSMIC) fleet started to provide GPS RO data (Anthes et al. [13]). A variety of studies have demonstrated that GPS RO measurements have a particularly positive impact on analyses and forecasts of temperature and humidity fields, even though the number of GPS RO observations is much lower than the number of satellite radiance observations assimilated (Healy et al. [14]; Healy and Thépaut [15]; Aparicio and Deblonde [16]; Poli et al. [10]; Cucurull [9]; Rennie [7]; Boinavita [17]; Liu et al. [12]). The significant positive impact of GPS RO observations on NWP is attributed to the all-weather, globally distributed measurements with high accuracy and relatively high vertical resolution (Ware et al. [18]; Kursinski et al. [19]). GPS RO observations can provide complementary information to that obtained from satellite radiances (Collard and Healy [20]). Another relevant feature of GPS RO observations is that their low systematic errors (Eyre [1]) allow them to be used without any bias correction, and they can be used as anchor points for the bias correction of radiance observations (Collard and Healy [20]; Dee [21]; Bauer et al. [22]; Cucurull et al. [23]).

Aging of the COSMIC fleet over recent years has considerably reduced the amount of occultation data available, which can degrade the skill of global NWP models (Von Engeln et. al. [24]). Fortunately, some new meteorological satellites, e.g., METOP-A and METOP-B, which carry the GPS RO instrument Global Receiver for Atmospheric Sounding (GRAS), were launched in 2006 and 2012, respectively. At that time, the GRAS receivers were the only fully operational GPS RO instruments (Bonavita [17]). They can provide around 1400 atmosphere profiles per day, mitigating the loss of data from the COSMIC fleet. Since

Received 2020-07-16 **Revised** 2020-08-15 **Accepted** 2020-11-15
Funding: National Key R&D Program of China (2018YFC1506205, 2018YFC1506702)
Biography: WANG Jin-cheng, Ph. D., primarily undertaking research on GNSS RO and satellite radiance data assimilation.
Corresponding author: HAN Wei, e-mail: hanwei@cma.gov.cn

September 23, 2013, atmospheric sounding has been carried out by the Global Navigation Satellite System Occultation Sounder (GNOS), a multi-GNSS (Global Navigation Satellite System) receiver that has the ability to receive and process both GPS and Chinese BeiDou navigation System (BDS) signals, on the Chinese new generation polar orbital satellite FY-3C. The GNOS produces up to 800 measurements per day. A previous study showed that GNOS possesses a sounding capability consistent with that of COSMIC and GRAS in the vertical range of 0−30 km, although it needs further improvement at higher altitudes (Liao et al. [25]). It is expected that the assimilation of GNOS data can positively impact NWP and improve forecast skill. In this work, we evaluate the impact of GNOS data on NWP by assimilating the GNOS GPS RO refractivity data within GRAPES (Global / Regional Analysis and PrEdiction System) 3D-Var (three-dimensional variational system), and analyze its impact on operational numerical weather forecasts. Only the GPS RO refractivity data are assimilated.

This paper is organized as follows. In section 1, the key characteristics of GNOS are briefly described. In section 2, a gross quality control scheme is introduced and the quality of GNOS data before assimilation is carefully evaluated using ECMWF reanalysis fields. In section 3, we detail the implementation of the GNSS RO refractivity assimilation method in GRAPES 3D-Var and the effect of the background check quality control on GNOS GPS RO refractivity. In section 4, the impacts of GNOS GPS RO refractivity assimilation on GRAPES analyses are illustrated. In section 5, the impact of GNOS GPS RO refractivity assimilation on forecasts is analyzed. We conclude with a summary and discussion in section 6.

2 BRIEF DESCRIPTIONS OF GNOS GPS RO OBSERVATIONS

GNOS is a multi-GNSS receiver that has the ability to track up to eight GPS satellites and four BDS satellites for precise orbit determination (Bi et al. [26]; Yang et al. [27]; Bai et al. [28]). In addition, it has velocity and anti-velocity antennas to simultaneously track up to six and four occultation events from GPS and BDS, respectively. These features enable GNOS to provide up to 800 atmosphere sounding profiles per day. More information on the GNOS instrument specifications can be found in Bai et al. [28].

GNOS is mounted on the Chinese FY-3C meteorological satellite, the first operational satellite in the FY-3 series (Yang et al. [27]), which was launched on September 23, 2013. According to the meteorological satellite program of China, GNOS will continue to be carried on FY-3C and follow-up platforms. GNOS on FY-3 series is expected to provide more and more RO measurements consistently until at least 2030.

Liao et al. [25] evaluated GNOS refractivity data quality based on the bias and standard deviation when compared against ECMWF re-analyses fields. The results of their study showed that GNOS possesses a sounding capability consistent with COSMIC and GRAS in the vertical range of 0−30 km.

The 3-month GNOS GPS RO refractivity data in boreal winter (December-February, DJF) of 2013/2014 were employed to develop and test the proposed gross QC procedure. They were also used to evaluate the impact on NWP forecasts. A total of 33,018 GPS RO profiles were received by GNOS in winter 2013/2014. Fig. 1 displays gridded binned averages of the lowest tangent point height on a rectilinear grid using the 33,018 GNOS RO profiles in winter 2013/2014, and the variation of the RO count with latitude. The GNOS GPS RO observations are distributed throughout the entire globe (Fig. 1a). More than 70% of the GNOS GPS RO events over the globe occurred in the middle latitudes (70° S to 20° S; 20° N to 70° N), and less than 16% occurred in the low latitudes (20° S to 20° N). Furthermore, nearly 78.4% of the ROs penetrated into the atmosphere below 2 km (Table 1). The lowest penetrating heights in the RO data over the tropical ocean and high mountains are typically higher than those over the subtropical ocean.

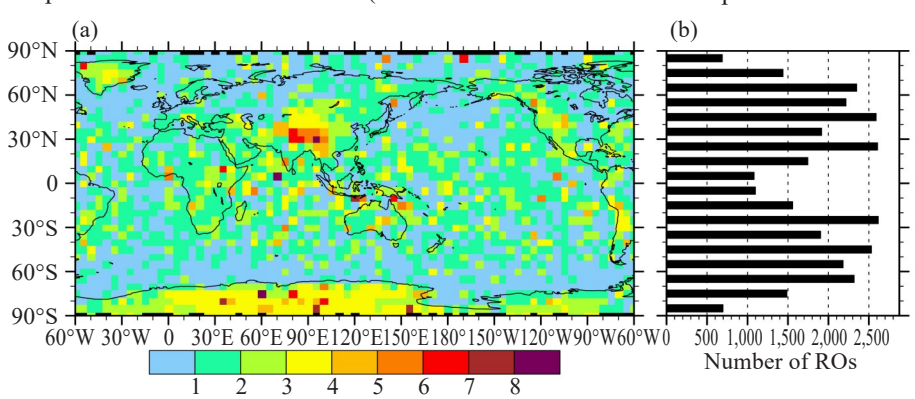

Figure 1. (a) Gridded binned averages of the lowest tangent point height on a rectilinear grid using the 33,018 GNOS RO profiles in winter 2013/2014. The latitude and longitude grid spacing is 5 degrees. (b) Histogram of the number of RO events in different 18-degree latitudinal bands.

Table 1. Data ratio (%) of the lowest tangent point heights.

H_b(km)	H_b<1.0	1.0≤H_b<2.0	2.0≤H_b<3.0	3.0≤H_b<4.0	4.0≤H_b<5.0	5.0≤H_b<6.0	6.0≤H_b<7.0	H_b>8.0	Total
Ratio (%)	60.7	17.7	9.8	5.5	2.2	1.4	0.8	1.9	100

3 GROSS QUALITY CONTROL OF GNOS REFRACTIVITY DATA

QC often has a large influence on the impact of observations on numerical weather forecasts (Rohn et al. [29]; Zou et al. [30]; Zou and Zeng [31]). Therefore, QC should be carefully carried out on GNOS GPS RO refractivity data before they are assimilated within NWP systems.

The GNOS GPS RO refractivity data quality was first assessed by comparing the data with ERA-Interim reanalysis fields. Fig. 2(a) demonstrates that the fractional refractivity of GNOS GPS ROs (i. e., the difference between the GNOS observed and ERA-Interim reanalysis simulated refractivity data) is often larger than 100%, which may imply that these GNOS GPS RO refractivity data are erroneous. These abnormal data were found to be related to GNOS GPS L2 signal tracking problems and the subsequent extrapolation of the L2 signal (Liao et al. [32]). From the left-hand panels of Fig. 3, which show scatter plots of refractivity against those calculated from ERA-Interim reanalysis, the abnormal observations can be clearly seen at the three different pressure levels (850 hPa, 500 hPa, and 200 hPa). These abnormal data must be distinguished and rejected to avoid them being assimilated into NWP. Therefore, gross quality control should be used immediately just after the RO events occur. However, the ERA-Interim reanalysis data are not ready at the observation time, meaning they cannot be used in the QC procedure.

To distinguish and reject outliers, a new gross quality control scheme, which includes a climate extreme check (CEC) and a vertical gradient check (VGC), is proposed for GNOS GPS RO refractivity data. In the first step, i. e., CEC, the whole profile is rejected if at any level the GNOS GPS RO refractivity data are larger (smaller) than the climate maximum (minimum) value from COSMIC (Fig. 4). In the VGC procedure, the data below the level with vertical gradient greater than zero are rejected. Fig. 4 shows vertical profiles of the climate maximum and minimum refractivity of COSMIC during 2013−2017 in different 30-degree latitudinal bands, which are used in the CEC.

After the gross quality control procedures, i. e., CEC and VGC, abnormal GNOS GPS RO refractivity data are distinguished and rejected. Fig. 2b shows that below 10 hPa the fractional refractivity after QC is less than 60% for all GNOS GPS RO profiles. The right-hand panels of Fig. 3 demonstrate that the scatter in the GNOS GPS RO refractivity data and the ERA-Interim reanalysis data are reasonable, which implies that the gross quality control scheme can effectively distinguish and remove abnormal data.

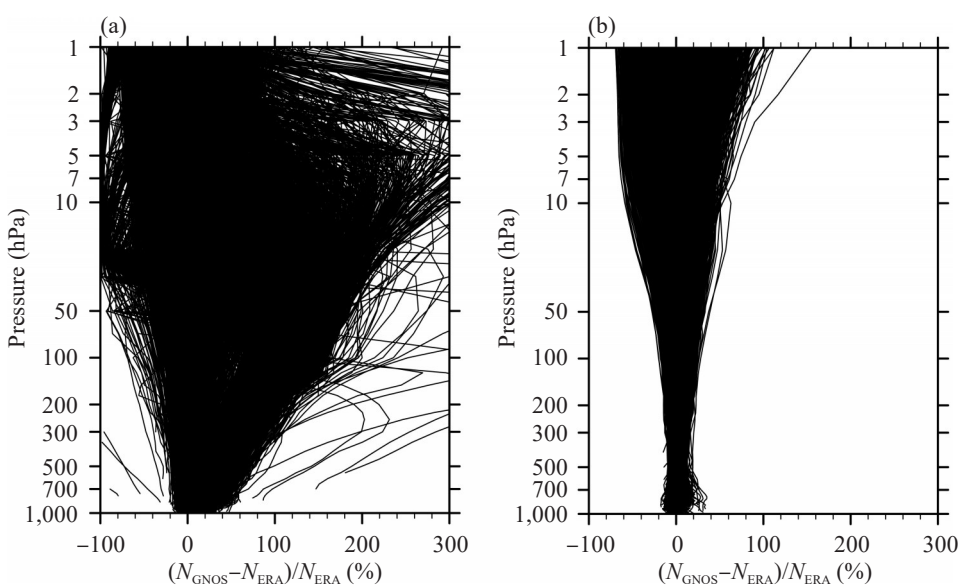

Figure 2. Normalized refractivity (%) of GNOS GPS RO observations (a) before and (b) after quality control against ERA-Interim estimates in DJF of 2013−2014.

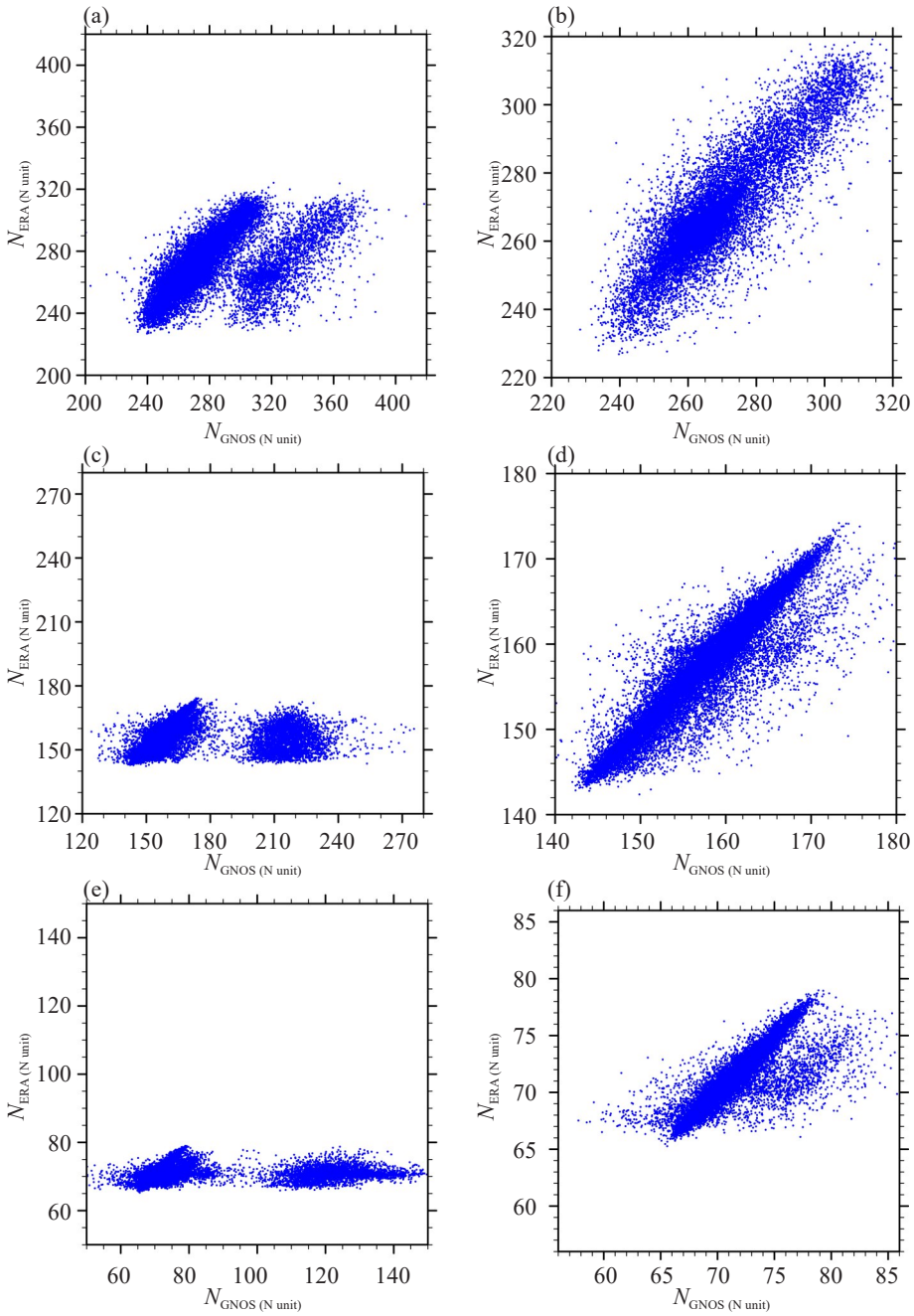

Figure 3. Scatter plots of GNOS refractivity against values calculated from ERA-Interim reanalysis at the (a, b) 850-hPa, (c, d) 500-hPa, and (e, f) 200-hPa pressure levels. Left-hand panels show results before QC, and right-hand panels show results after QC.

The variational assimilation method requires that the probability distribution function (PDF) of observational data is Gaussian (Lorenc [33]). Fig. 5 shows PDFs of GNOS GPS RO fractional refractivity at the 850-hPa, 500-hPa, and 200-hPa pressure levels before and after gross quality control. Before gross quality control, the PDFs of fractional refractivity at all three pressure levels have two peaks, i.e., a main peak and a smaller peak of abnormal data. After gross quality control, the PDFs of fractional refractivity have near-Gaussian distributions. These results imply that gross quality control is an effective method for recognizing and removing abnormal GNOS GPS RO data.

Table 2 shows that over 35% of the refractivity data, a larger proportion than in the other domains, is rejected in the low-latitude bands (30°S to 0, and 0 to 30° N) where the numbers of GNOS GPS RO observations are the lowest (Fig. 1b). These results suggest that the abnormal observations may be related to humidity (Liao et al. [32]). Over the whole globe, 21.2% of refractivity data was determined to be erroneous in the gross quality control, which is a considerable proportion. Liao et al. [32] found that these

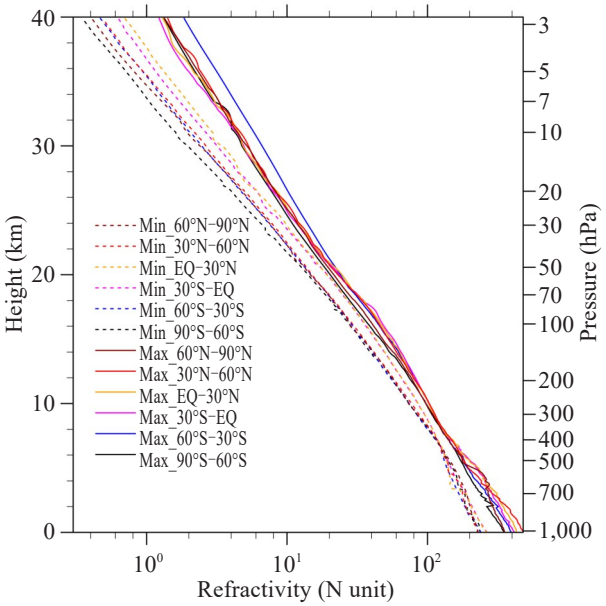

Figure 4. Vertical profiles of the climate maximum (solid lines) and minimum (dashed lines) refractivity (units: N unit) in COSMIC data for 2013–2017 in different 30-degree latitudinal bands.

large biases are related to L2 signal degradation, and proposed a new extrapolation procedure to improve the L2 extrapolation of GNOS which eliminates about 90% of the large departure profiles. For more information please refer to Liao et al. [32].

The mean and standard deviation of fractional refractivity before and after gross quality control were calculated for the different latitude bands of both hemispheres. Near the 100-hPa pressure level, the standard deviations of fractional refractivity before gross quality control are larger than 25% for all latitude bands (Fig. 6). Before gross quality control, not only the standard deviation of fractional refractivity, but also the positive mean for all pressure levels and domains are very large. After gross quality control, the means of fractional refractivity in different domains are reduced significantly, becoming almost zero below 10 hPa. The standard deviation values are also significantly decreased, and are comparable with those of COSMIC and GRAS. These standard deviations of fractional refractivity after gross quality control were set as the GNOS refractivity observational errors in GRAPES 3D-Var.

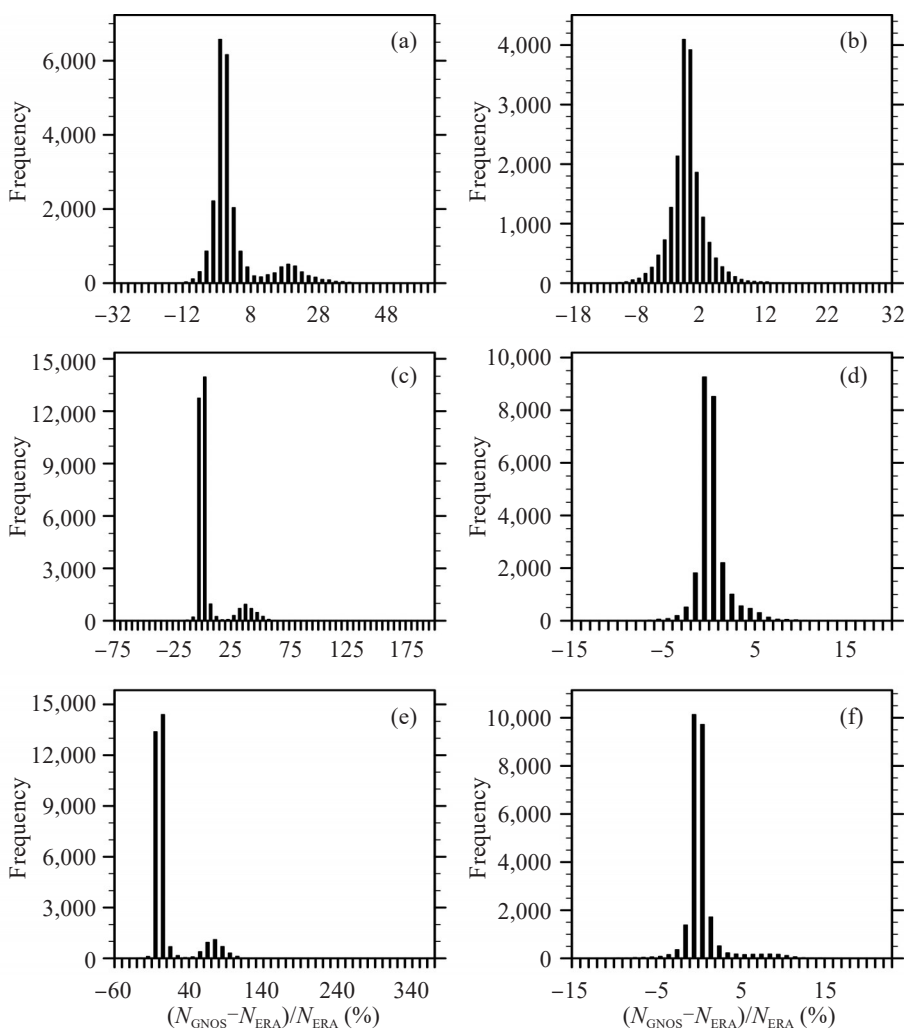

Figure 5. Probability distribution functions of GNOS fractional refractivity at the (a, b) 850-hPa, (c, d) 500-hPa, and (e, f) 200-hPa pressure levels. Left-hand panels show results before QC, and right-hand panels show results after QC.

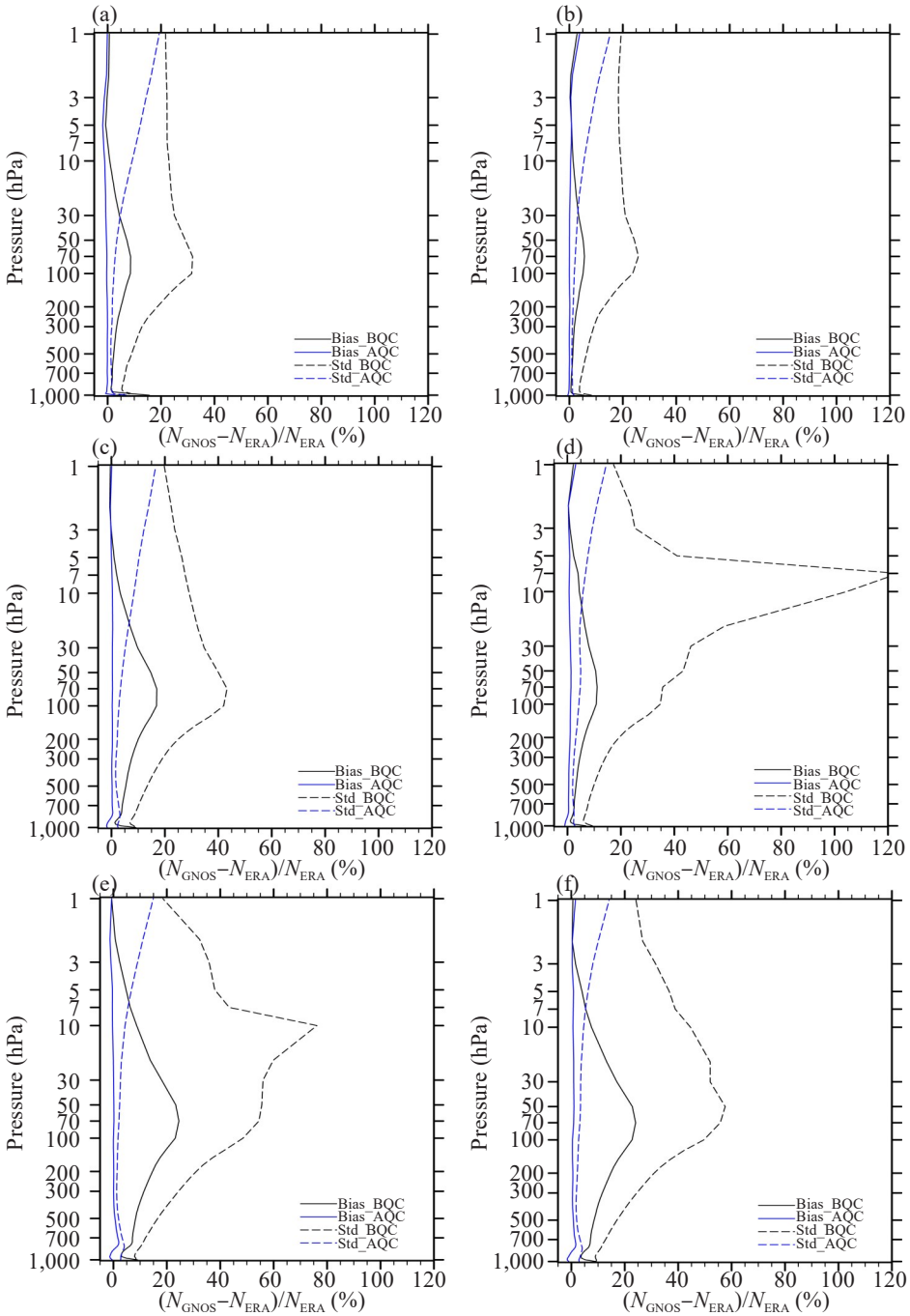

Figure 6. Vertical profiles of the mean (solid curves) and standard deviation (dashed curves) of the difference between the GNOS-observed and ERA-Interim reanalysis simulated refractivity data before (black curves) and after (blue curves) gross quality control in the (a, b) high-latitude and (c, d) mid-latitude extratropics, and (e, f) the tropics of the Southern Hemisphere (left-hand panels) and Northern Hemisphere (right-hand panels).

Table 2. The number of GNOS GPS RO observations before and after gross QC in different latitudinal bands and over the whole globe.

Domain	Before QC	After QC	Rejected	Ratio of outliers (%)
(90°S–60°S)	135,347	119,069	16,278	12.0
(60°S–30°S)	215,873	171,059	44,814	20.7
(30°S–0)	167,760	107,431	60,329	35.9
(0–30°N)	170,557	106,727	63,830	37.4
(30°N–60°N)	213,607	185,673	27,933	13.1
(60°N–90°N)	142,696	134,009	8,686	6.1
Globe	1,045,840	823,968	221,872	21.2

4 IMPLEMENTATION OF GNOS GPS RO REFRACTIVITY ASSIMILATION

GRAPES is the Chinese new generation operational NWP system (Xue [34]; Xue et al. [35]). The global GRAPES version with 3D-Var on terrain-following height vertical coordinates, which is the same as the GRAPES forecast model (Xue et al. [36]), has been applied to routine operation in the National Meteorological Center of the China Meteorological Administration (CMA).

GNSS RO refractivity data have routinely been assimilated in the GRAPES 3D-Var system since 2014. A preliminary assessment of the GNSS RO refractivity data demonstrated that the data have a significant positive effect on analyses and forecasts in all regions, especially in the Southern Hemisphere extratropics and the global stratosphere. GNSS RO data have become one of the most important types of observation in GRAPES (Liu and Xue [12]).

Besides the gross quality control outlined in section 2, the preprocessing procedure for RO data involves thinning of refractivity data in the vertical direction, since the vertical resolution of the occultation data is much higher than that of the model. The observations nearest the model levels are selected for assimilation.

The background check is applied to the GNSS RO data to remove outliers in the GRAPES 3D-Var system. The criterion used in the background check is

$$\left| N_o - N_b \right| > 4\delta_o \tag{1}$$

where the subscripts o and b represent the observation and background, N is the refractivity in N-units, and δ_o is the standard deviation of observational error. This check was chosen for the GNOS GPS RO data as same as other GPS RO observations (Liu and Xue [12]). After the background check, the probability distribution functions of refractivity OMB (the difference between observed refractivity and simulated refractivity by the GRAPES background) at model levels 14, 25 and 40 are closer to a Gaussian distribution (Fig. 7).

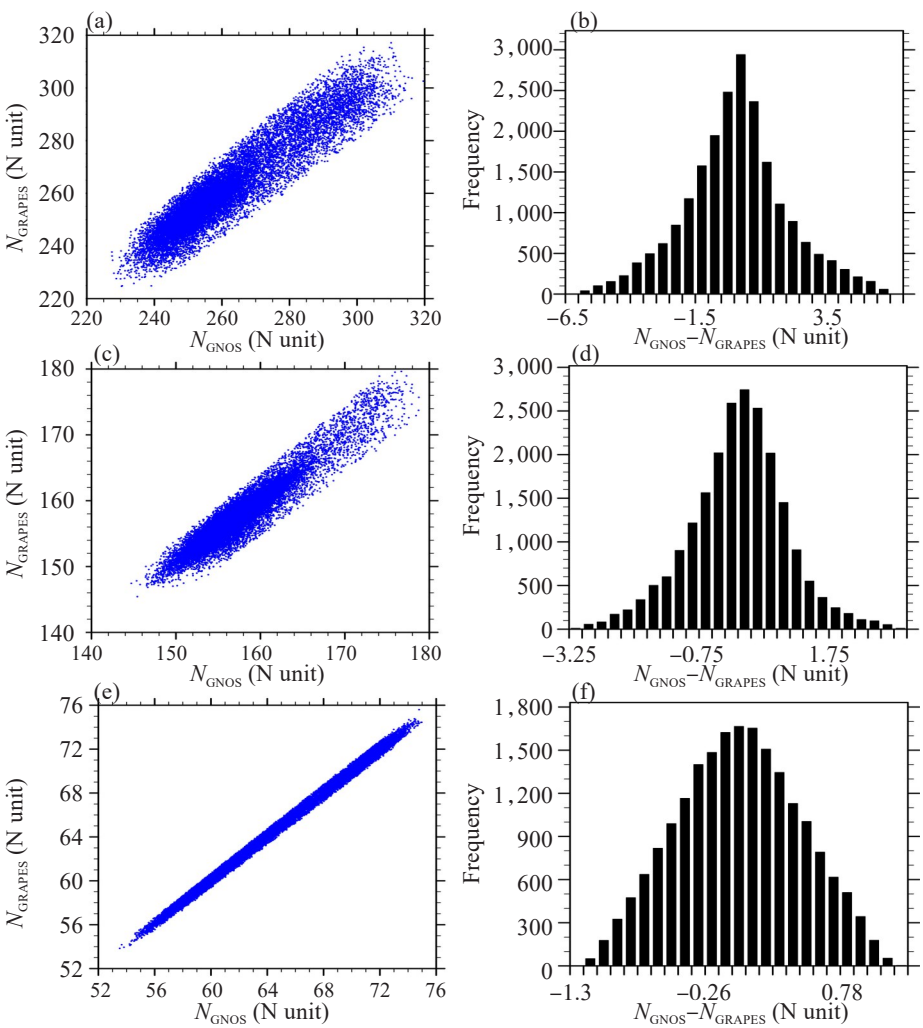

Figure 7. (a, c, e) Scatter plots of GNOS-observed refractivity and refractivity calculated from the GRAPES background fields, and (d, e ,f) probability distribution functions of GNOS refractivity values minus the GRAPES background simulated values (OMB) after the background check for GRAPES model levels (a, b) 14, (c, d) 25, and (e, f) 40, which correspond to approximately 850 hPa, 500 hPa and 200 hPa, respectively.

The observation operator of GNSS RO refractivity in the GRAPES assimilation system is still the local refractivity operator expressed as

$$N = 77.6\frac{P}{T} + 3.73 \times 10^5 \times \frac{P_e}{T^2}, \quad (2)$$

where N is the refractivity in N-units, P is the atmosphere pressure in hPa, T is the atmosphere temperature in Kelvin, and P_e is the water vapor pressure in hPa. Further details about the assimilation of GNSS RO refractivity data in the GRAPES assimilation system can be found in Liu and Xue [12].

5 EXPERIMENTS SETUP AND IMPACT ON ANALYSIS

To assess the impact of GNOS RO refractivity data on GRAPES analysis and forecast, two experiments with and without assimilation of GNOS RO refractivity data were set up and run for one winter period (1 December, 2013 to 28 February, 2014). They are called as the control experiment (CTRL) and GNOS data assimilation experiment (GNOS), respectively. CTRL includes all operationally available conventional observations, Atmospheric Motion Vectors (AMVs) from geostationary and polar orbiting satellites, radiance data from AMSU-A on NOAA-15, NOAA-17/19, Metop-A and Metop-B, and all the GPS RO refractivity data available operationally (e.g., those from COSMIC and GRAS) except for the GNOS refractivity data. GNOS assimilates all of the observations in CTRL plus GNOS GPS RO observations over the globe during the whole experiment period. GRAPES forecast system version 2.1.1.1 was employed for these experiments. The horizontal resolution of both the outer-loop and inner-loop was 0.5 degrees in both experiments, and the time window length of 3D-Var was 6 hours. The model top was 36.4 km, with 60 layers. The time integration step was 600 seconds and the horizontal resolution was 0.5 degrees.

A first look at the impact of GNOS RO data on the GRAPES analysis can be obtained by comparing the departure of the observation from the background and analysis (OMB and OMA, respectively). Fig. 8 shows the profiles of the mean and standard deviation of (O−B)/O and (O−A)/O for GNOS GPS refractivity in GNOS in the tropics, NH extratropics, and SH extratropics. The mean profiles of (O−A)/O are much closer to zero than those of (O−B)/O, and the standard

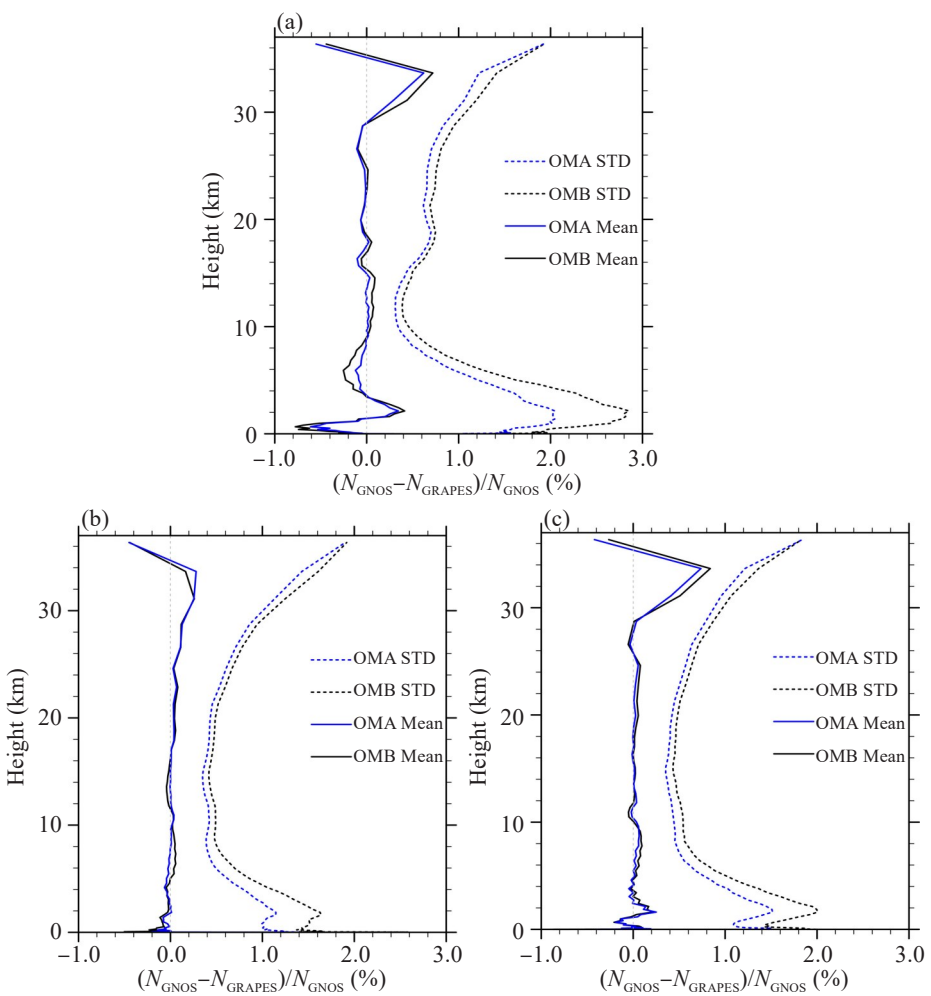

Figure 8. Plots of mean (solid lines) and standard deviation (dashed lines) profiles of (O−B)/O (black lines) and (O−A)/O (blue lines) for GNOS refractivity in (a) the tropics, the (b) NH and (c) SH extratropics.

deviation profiles of (O−A)/O are significantly reduced in all domains compared with those for (O − B)/O. These results imply that the specified observational error is reasonable, and the assimilation of GNOS GPS RO refractivity data has a clear positive effect on the analysis.

National Centers for Environmental Prediction (NCEP) final (FNL) analysis data are considered more precise than GRAPES analysis data because much more satellite remote sensing data is assimilated in FNL. We therefore used FNL data as the reference state of the atmosphere to evaluate the impact of GNOS GPS RO observation assimilation. Fig. 9 shows the normalized average of the root-mean-squared-error (RMSE) reduction rate of the GRAPES temperature analyses after GNOS GPS data assimilation during the DJF period. These results illustrate that analysis errors in the temperature fields are significantly reduced by more than 1%, except at the 20-hPa and 1000-hPa levels in the SH. The analysis error of temperature at the 300-hPa pressure level in the SH is decreased by more than 1.5%. Note that the number of GNOS GPS RO values assimilated was 1,065,155 during the whole experiment, which is only about 10.7% of the other GPS RO data and approximately 0.6% of all assimilated observations.

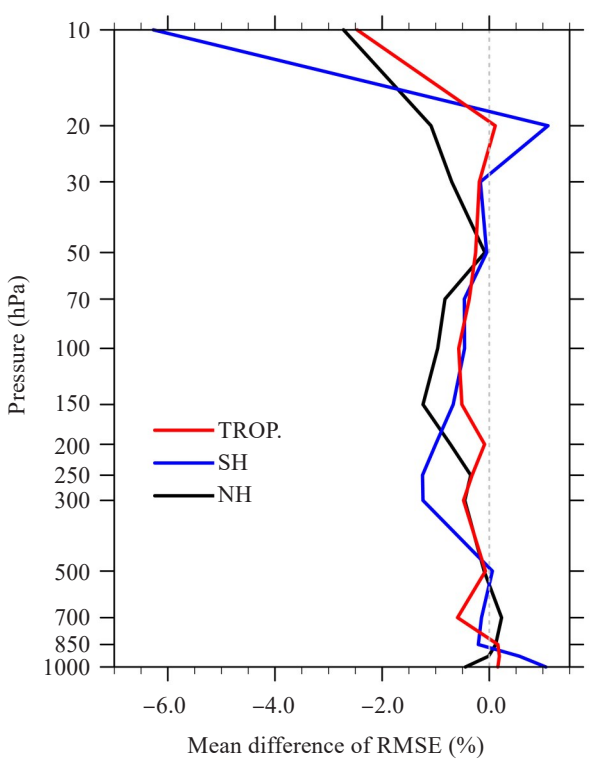

Figure 9. Normalized average of the root-mean-squared-error reduction of the GRAPES temperature analyses in the tropics (red line), SH (blue line) and NH (black line), after GNOS GPS RO data assimilation during winter 2013/2014. The reference temperature fields are from NCEP FNL.

6 IMPACT ON FORECASTS

The impact of the additional information provided by the GNOS GPS RO data on forecasts is illustrated in Fig. 10, which shows zonal means of the standard deviation of the difference in the temperature fields between experiments GNOS and CTRL for the winter period at different forecast times (T+0h, T+24h, T+48h, and T+72h).

As expected, the impact on the temperature analysis (Fig. 10a) is mainly seen in the stratosphere (above 250 hPa). However, a similar impact is found in the SH troposphere. The impact of assimilating GNOS GPS RO data is larger in the SH troposphere than in the NH troposphere because the number of conventional observation profiles from aircraft reports and radiosondes in the SH troposphere is only approximately five percent of the number available in the NH.

The impact on the analysis in the SH is considerable in the middle to higher troposphere. These impacts are enhanced in the subsequent forecasts (Fig. 10b-d), expanding and strengthening throughout the SH troposphere and lower stratosphere. In the SH, the GNOS GPS RO data complement the conventional observation network and other GPS RO observation networks, both in the troposphere and the stratosphere.

In the tropics, the impact on the analysis is larger above 150 hPa, roughly the height of the tropopause. The analysis perturbations appear to downwards and towards higher latitudes, so after 3 days most of the NH is affected.

Figure 11 shows time series of the anomaly correlation coefficient (ACC) of geopotential height on 250 hPa and 500 hPa over the SH and NH out to 240 h (10 days) from 1 December 2013 to 28 February 2014 in both CTRL and GNOS. In the NH, ACC increases slightly with forecast time at 250 hPa and 500 hPa, but turns negative at 500 hPa on day 9. The increase in AAC is much larger in the SH, and becomes significant at 500 hPa on day 9.

7 SUMMARY AND DISCUSSION

In this study, a gross quality control procedure has been proposed and applied to GNOS GPS RO refractivity data. It consists of a climate extreme check and a vertical gradient check. The procedure can effectively identify outliers in GNOS GPS refractivity data. After QC, which removes 21% of GNOS GPS RO refractivity data as outlier, the data is closer to the ERA-Interim reanalyses than the original data, resulting in improved spatial consistency, a more symmetric probability distribution, and significantly reduced error variance and bias.

The quality-controlled GNOS GPS RO refractivity data are assimilated in GRAPES 3D-Var. Results of an

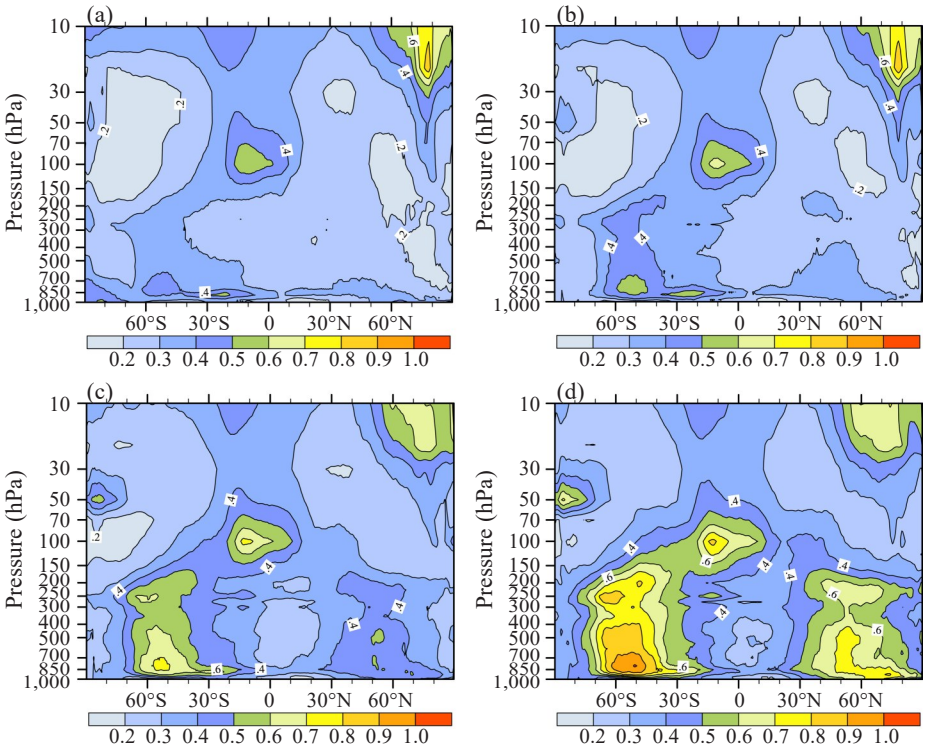

Figure 10. Zonal means of the standard deviation of the difference in the temperature field between CTRL and GNOS for DJF 2013/2014 at forecast times (a) T+0h, (b) T+24h, (c) T+48h, and (d) T+72h.

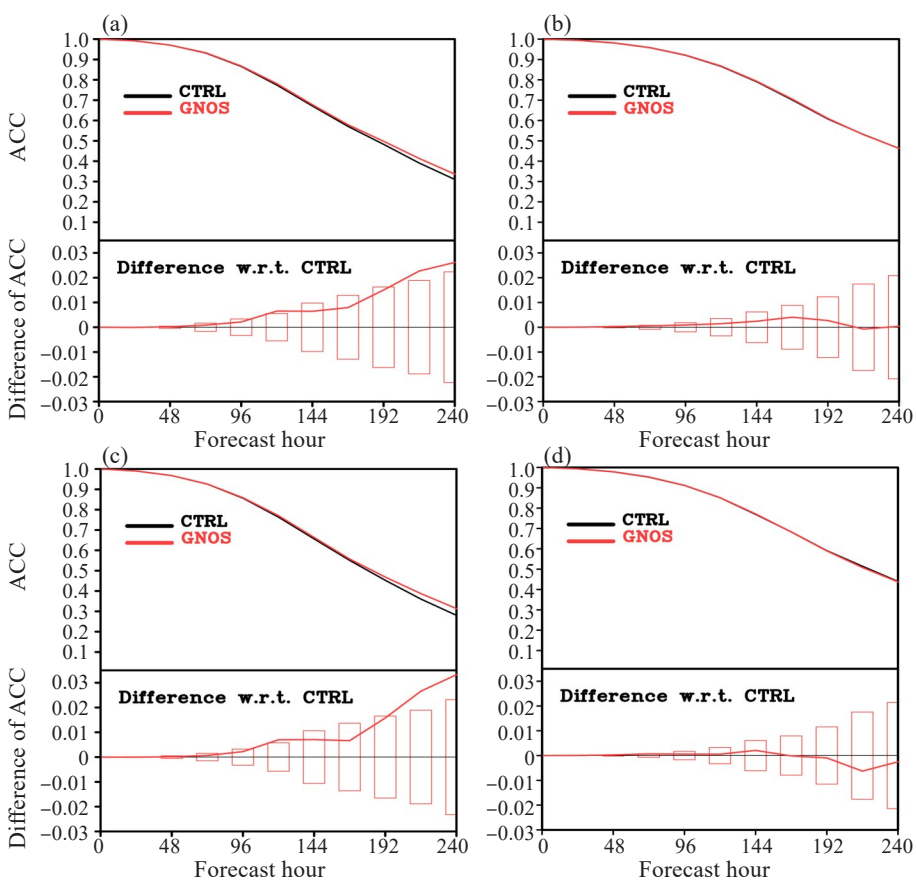

Figure 11. Time series of averaged anomaly correlation scores (ACC) of geopotential height in CTRL (black lines) and GNOS (red lines) over the (a, c) SH and (b, d) NH at (a, b) 250 hPa and (c, d) 500 hPa during the forecast period from 1200 UTC on 1 December 2013 to 1200 UTC on 28 February 2014. The bottom panel of each subplot shows the difference in ACC between GNOS and CTRL, with positive values indicating improvement. The bars illustrate the 95% confidence intervals; values located outside the bars are statistically significant.

experiment run over one whole winter season show a positive impact of GNOS GPS RO data on both the analysis and forecast, especially in the SH. The RMSE of analysis temperature is reduced by more than 1% in the SH and tropics, and the anomaly correlation scores of the 250- and 500-hPa geopotential height forecasts over the SH increase significantly from days 1 to 5. Supported by these encouraging results, GNOS GPS RO data have been assimilated in GRAPES 3D-Var since June 1, 2016 at the National Meteorological Center of the China Meteorological Administration.

Currently, only the GPS RO refractivity of GNOS is assessed and assimilated in GRAPES 3D-Var, even though GNOS also provides BDS RO data. In the near future, GNOS BDS RO refractivity data will be evaluated and assimilated in GRAPES.

Acknowledgements: The authors are thankful to the National Satellite Meteorological Center of CMA for providing GNOS RO data.

REFERENCES

[1] EYRE J R. Assimilation of radio occultation measurements into a numerical weather prediction system [EB / OL]. (1994) [2020-10-21]. https://www.ecmwf.int/node/9331.

[2] CUCURULL L, DERBER J C, PURSER R J. Assimilation of global positioning system radio occultation observations into NCEP's Global Data Assimilation System [J]. Mon Wea Rev, 2007, 135(9): 3174-3193, https://doi.org/10.1175/MWR3461.1.

[3] CUCURULL L, DERBER J C. Operational implementation of COSMIC observations into the NCEP's Global Data Assimilation System [J]. Wea Forecasting, 2008, 23(4): 702-711, https://doi.org/10.1175/2008WAF2007070.1.

[4] CUCURULL L, DERBER J C, PURSER R J. Preliminary impact studies using global positioning system radio occultation profiles at NCEP [J]. Mon Wea Rev, 2008, 136 (6): 1865-1877, https://doi.org/10.1175/2007MWR2260.1.

[5] BUONTEMPO C, JUPP A, RENNIE M P. Operational NWP assimilation of GPS radio occultation data [J]. Atmos Sci Lett, 2008, 9(3): 129-133, https://doi. org / 10.1002 / asl.173.

[6] ANLAUF H, PINGEL D, RHODIN A. Assimilation of GPS radio occultation data at DWD [J]. Atmos Meas Tech, 2011, 4: 1105-1113, https://doi. org / 10.5194 / amt-4-1105-2011.

[7] RENNIE M P. The impact of GPS radio occultation assimilation at the Met Office [J]. Quart J Roy Meteor Soc, 2010, 136(646): 116-131, https://doi.org/10.1002/qj.521.

[8] HEALY S B. Forecast impact experiment with a constellation of GPS radio occultation receivers [J]. Atmos Sci Lett, 2008, 9(3): 111-118, https://doi. org / 10.1002 / asl.169.

[9] CUCURULL L. Improvement in the use of an operational constellation of GPS radio occultation receivers in weather forecasting [J]. Mon Wea Rev, 2010, 25(2): 749-767, https: //doi.org/10.1175/2009WAF2222302.1.

[10] POLI P, MOLL P, PUECH D, et al. Quality control, error anlaysis, and impact assessment of FORMOSAT-3 / COSMIC in numercial weather prediction [J]. Terr Atmos Oceanic Sci, 2009, 20: 101-113, https://doi.org / 10.3319 / TAO.2008.01.21.02(F3C).

[11] CARDINALI C, HEALY S. Impact of GPS radio occultation measurements in the ECMWF system using adjoint-based diagnostics [J]. Quart J Roy Meteor Soc, 2014, 140: 2315-2320, https://doi.org/10.1002/qj.2300.

[12] LIU Y, XUE J S. Assimilation of global navigation satellite radio occultation observations in GRAPES: Operational implementation [J]. J Meteorol Res-Prc, 2014, 28(6): 1061-1074, https://doi. org / 10.1007 / s13351-014-4027-1.

[13] ANTHES R A, BERNHARDT P A, CHEN Y, et al. The COSMIC / FORMOSAT-3 mission: Early results [J]. Bull Amer Meteor Soc, 2008, 89(3): 313-333, https://doi. org / 10.1175/BAMS-89-3-313.

[14] HEALY S B, JUPP A, MARQUARDT C. Forecast impact experiment with GPS radio occultation measurements [J]. Geophys Res Lett, 2005, 32(3): L03804, https://doi. org / 10.1029/2004GL020806.

[15] HEALY S B, THÉPAUT J N. Assimilation experiments with CHAMP GPS radio occultation measurements [J]. Quart J Roy Meteor Soc, 2006, 132(615): 605-623, https:// doi.org/10.1256/qj.04.182.

[16] APARICIO J M, DEBLONDE J. Impact of the assimilation of CHAMP refractivity profiles in Environment Canada global forecasts [J]. Mon Wea Rev, 2008, 136(1): 257-275, https://doi. org / 10.1175 / 2007MWR1951.1.

[17] BONAVITA M. On some aspects of the impact of GPSRO observations in global numerical weather prediction [J]. Quart J Roy Meteor Soc, 2014, 140(685): 2546-2562, https://doi.org/10.1002/qj.2320.

[18] WARE R, ROCKEN C, SOLHEIM F, et al. GPS sounding of the atmosphere from low earth orbit: Preliminary results [J]. Bull Amer Meteor Soc, 1996, 77(1): 19-40, https://doi. org / 10.1175 / 1520-0477(1996)077<0019: GSOTAF>2.0.CO;2.

[19] KURSINSKI E R, HAJJ G A, HARDY K R, et al. Observing Earth's atmosphere with radio occultation measurements [J]. J Geophys Res, 1997, 102(D19): 23429-23465, https://doi.org/10.1029/97JD01569.

[20] COLLARD A D, HEALY S. The combined impact of future space-based atmospheric sounding instruments on numerical weather predicition analysis fields: A simulation study [J]. Quart J Roy Meteor Soc, 2003, 129 (593): 2741-2760, https://doi.org/10.1256/qj.02.124.

[21] DEE D P. Bias and data assimilation [J]. Quart J Roy Meteor Soc, 2005, 131(613): 3323-3343, https://doi. org / 10.1256/qj.05.137.

[22] BAUER P, RADNÓTI G, HEALY S, et al. GNSS radio occulation constellation observing sytem experiments [J]. Mon Wea Rev, 2014, 142(2): 555-572, https://doi. org / 10.21957/je1yremu.

[23] CUCURULL L, ANTHES R A, TSAO L-L. Radio occultation observations as Anchor Observations in numerical weather prediction models and associated reduction of bias corrections in microwave and infrared satellite observations [J]. J Atmos Oceanic Technol, 2014, 31(1): 20-32, https://doi. org / 10.1175 / JTECH-D-13-00059.1.

[24] VON ENGELN A, HEALY S, MARQUARDT C, et al. Validation of operational GRAS radio occultation data [J]. Geophys Res Lett, 2009, 36(17): L17809, https://doi.org/10.1029/2009GL039968.

[25] LIAO M, ZHANG P, YANG G L, et al. Preliminary validation of refractivity from a new radio occultation sounder GNOS / FY-3C [J]. Atmos Meas Tech, 2016, 9: 781-792, https://doi.org/10.5194/amtd-8-9009-2015.

[26] BI Y M, YANG Z D, ZHANG P, et al. An introduction to China FY3 radio occultation mission and its measurement simulation [J]. J Adv Space Res, 2012, 49(7): 1191-1197, https://doi.org/10.1016/j.asr.2012.01.014.

[27] YANG J, ZHANG P, LU N M, et al. Improvements on global meteorological observations from the current Fengyun 3 satellites and beyond [J]. Int J Digital Earth, 2012, 5(3): 1-15, https://doi. org / 10.1080 / 17538947.2012.658666.

[28] BAI W H, SUN Y Q, DU Q F, et al. An introduction to the FY3 GNOS instument and mountain-top tests [J]. Atmos Meas Tech, 2014, 7: 1817-1823, https://doi.org/10.5194/amt-7-1817-2014.

[29] ROHN M, KELLY G, SAUNDERS R. Experiments with Atmospheric Motion Vectors at ECMWF [C]//Proc of Fourth International Winds Workshop, Saanenmoser (Switzerland): EUMETSAT, 1998: 139-146.

[30] ZOU X, LIU H, ANTHES R A, et al. Impact of CHAMP radio occultation observations on global analysis and forecasts in the absence of AMSU radio data [J]. J Meteorol Soc Japan, 2004, 82(1B): 533-549, https://doi.org/10.2151/jmsj.2004.533.

[31] ZOU X, ZENG Z. A quality control procedure for GPS radio occultation data [J]. J Geophys Res, 2006, 111(D2): D02112, https://doi.org/10.1029/2005JD005846.

[32] LIAO M, HEALY S, ZHANG P. Processing and quality control of FY-3C GNOS data used in numerical weather prediction applications [J]. Atmos Meas Tech, 2019, 12: 2679-2692, https://doi.org/10.5194/amt-12-2679-2019.

[33] LORENC A. Analysis methods for numerical weather prediction [J]. Quart J Roy Meteor Soc, 1986, 112(474): 1177-1194, https://doi.org/10.1002/qj.49711247414.

[34] XUE Ji-shan. Progress of Chinese numerical prediction in the early new century [J]. J Appl Meteor Sci, 2006, 17: 602-610(in Chinese).

[35] XUE J S, ZHUANG S Y, ZHU G F, et al. Scientific design and preliminary results of three dimensional variational data assimilation system of GRAPES [J]. Chin Sci Bull, 2008, 53: 3446-3457.

[36] XUE Ji-shan, LIU Yan, ZHANG Lin. Scientific Documentation of GRAPES-3DVar Version for the Global Model [R]. Beijing: Numerical Weather Prediction Center, China Meteorological Administration, 2012(in Chinese).

Citation: WANG Jin-cheng, GONG Jian-dong, and HAN Wei. The impact of assimilating of FY-3C GNOS GPS radio occultation observations on GRAPES forecasts [J]. J Trop Meteor, 2020, 26(4): 390-401, https://doi.org/10.46267/j.1006-8775.2020.034.